

Article

Removal of Phosphorus and Cadmium from Wastewaters by Periphytic Biofilm

Jin Zhang ^{1,2}, Yawei Liu ^{1,2}, Jiajia Liu ³, Yu Shen ^{1,2}, Hui Huang ^{1,2}, Yongli Zhu ^{1,2}, Jiangang Han ^{1,2,*} and Haiying Lu ^{1,2,*}

¹ Co-Innovation Center for Sustainable Forestry in Southern China, College of Biology and the Environment, Nanjing Forestry University, Nanjing 210037, China; jinzhang@njfu.edu.cn (J.Z.); ywliu@njfu.edu.cn (Y.L.); shenyu@njfu.edu.cn (Y.S.); huanghui@njfu.edu.cn (H.H.); yonglizhu@njfu.edu.cn (Y.Z.)

² National Positioning Observation Station of Hung-tse Lake Wetland Ecosystem in Jiangsu Province, Nanjing 210037, China

³ Environmental Engineering College, Nanjing Polytechnic Institute, Nanjing 210044, China

* Correspondence: jianganghan@njfu.edu.cn (J.H.); luhaiying@njfu.edu.cn (H.L.)

Abstract: Phosphorus (Pi) and cadmium (Cd) contamination in water sources pose significant health risks and environmental concerns. Periphytic biofilms have been recognized for their ability to effectively remove these contaminants from aquatic environments. This study aimed to investigate the impact of photon and electron treatments on Pi and Cd removal by periphytic biofilms. The experiments spanned a monthly timeframe, focusing on how photon and electron treatments affected the contaminant removal efficiency of periphytic biofilms. The results revealed that while the introduction of electrons had a minimal impact on contaminant accumulation, the enhancement of photon exposure significantly improved the absorption capacity of periphytic biofilms. This, in turn, led to enhanced removal of Pi and Cd from the water. One possible explanation for this phenomenon is that photons played a crucial role in inducing nitrate and ammonium conversion, thereby facilitating the accumulation of 4.70 mg kg⁻¹ Pi and 2.40 mg kg⁻¹ Cd in periphytic biofilms. In contrast, electron treatment had limited effects on nitrate conversion. These findings provide valuable insights into the mechanisms underlying the removal of water contaminants by periphytic biofilms under the influence of electron and photon treatments. Furthermore, they have practical implications for improving pollutant removal capabilities in aquatic ecosystems using periphytic biofilms.

Keywords: periphytic biofilm; phosphorus; cadmium; photon; electron



Citation: Zhang, J.; Liu, Y.; Liu, J.; Shen, Y.; Huang, H.; Zhu, Y.; Han, J.; Lu, H. Removal of Phosphorus and Cadmium from Wastewaters by Periphytic Biofilm. *Water* **2023**, *15*, 3314. <https://doi.org/10.3390/w15183314>

Academic Editors: Laura Bulgariu and Hassimi Abu Hasan

Received: 3 August 2023

Revised: 14 September 2023

Accepted: 16 September 2023

Published: 20 September 2023



Copyright: © 2023 by the authors. Licensee MDPI, Basel, Switzerland. This article is an open access article distributed under the terms and conditions of the Creative Commons Attribution (CC BY) license (<https://creativecommons.org/licenses/by/4.0/>).

1. Introduction

Cadmium (Cd) is a well-established human carcinogen, and prolonged exposure to it can result in renal damage, bone demineralization, and an elevated risk of cancer, as documented in numerous studies [1,2]. The rapid pace of industrialization has led to widespread contamination of Cd in water bodies worldwide, with some regions in China experiencing particularly severe contamination, as reported by the World Health Organization (WHO) [3]. According to national soil pollution surveys, approximately 19.4% of the agricultural soils in China are contaminated, and among all contaminants, Cd exceeds acceptable levels in more than 7% of these cases [4]. Moreover, research has indicated a strong correlation between Cd uptake and the transfer of phosphorus (Pi) at the plant–soil interface [5]. This is exacerbated by the substantial influx of Pi into water bodies, such as lakes and rivers, stemming from various sources including agricultural runoff, wastewater discharge, and erosion from high-Pi soil [6]. As a result, the complex issue of Cd and Pi pollution in natural water environments has become a major concern.

Periphytic biofilm is a term used to describe a complex community of microorganisms, including algae, bacteria, fungi, and protozoa, that attach and grow on surfaces in aquatic environments [7]. It has been documented that periphytic biofilms are highly

effective in the removal of contaminants from aquatic environments [8]. For example, research has shown that periphytic biofilms can remove 0.27 g m^{-2} Pi, 9.26 mg m^{-2} As, 255.3 mg m^{-2} Cr, and 238.6 mg m^{-2} Zn per day [9]. Additionally, Lu et al. (2020) observed that periphytic biofilms significantly reduce Cd accumulation in rice, with a Cd adsorption rate of $390 \text{ pmol cm}^{-2} \text{ s}^{-1}$ [10]. Furthermore, when applied in wastewater treatment, periphytic biofilms have exhibited a high tolerance to Cu concentrations exceeding 2 mg L^{-1} [11]. By absorbing and accumulating Cd and Pi, periphytic biofilms effectively remove these contaminants from the water, reducing their availability to other organisms [12]. Therefore, it is imperative to understand the underlying mechanisms that drive periphytic biofilms' capacity to remove Cd and Pi from aquatic environments.

Nitrate serves as a crucial nitrogen source for periphytic biofilm [13], and the conversion of nitrate holds significant importance in providing nitrogen for physiological regulation and adaptation to stress. This process ensures the normal growth and development of plants, which, in turn, is vital for the overall development of plants [14]. Notably, light (photons) plays a pivotal role in nitrate conversion, with dark conditions reducing the cell growth by 4 to 5 pM per day compared to well-illuminated conditions in algae [15]. Moreover, the wavelength of light has been found to influence the efficiency of nitrate conversion, with the optimum wavelength being 510 nm, a major component of visible light [16]. It has been suggested that photons can enhance contaminant removal in periphytic biofilms. Furthermore, considering the photoelectric effect, both photons and electrons play roles in this process [17]. Electrons may also have the potential to improve nitrate conversion [18]. The interplay between photons and electrons in contaminant removal is not yet fully understood. There is existing research indicating that photons and electrons play important roles in plant growth [19], and growing periphytic biofilms exhibit a strong potential for contaminant removal [20]. Therefore, we aim to investigate whether the addition of photons and electrons could enhance the removal of Cd by periphytic biofilms. Simultaneously, periphytic biofilms play a role in removing Pi from aquatic environments, incorporating it into their biomass through processes like adsorption and precipitation [21]. This makes them an effective tool for managing eutrophication and water pollution [22]. In light of these considerations, our hypothesis is that photons and electrons may be key contributors to nitrate conversion, thus improving the removal of contaminants by periphytic biofilms.

In periphytic biofilm, environmental factors play a crucial role in nitrate conversion. For instance, it was discovered that nitrogen decline increased periphytic biofilm biomass by over 50% and induced compositional changes irrespective of water temperature and electrical conductivity (EC) in the shallow lakes, Central Jutland, Denmark [23]. In the Illinois River Watershed, it was reported that the periphytic biofilm nitrogen metabolism presents stronger relationships with pH. The pH would be higher than 9.2 when the nitrogen metabolism is limited, due to the smaller habit of the acquiring plants compared to plants with larger habit [24]. Therefore, in this study, we investigated the responses of the water temperature, EC, pH, etc., as these environmental factors of photons and electrons are the most sensitive to the improvement of the periphytic biofilm hydrophytic habitat. As a feedback, water temperature, EC, and pH are the major factors for periphytic biofilm to remove contaminants in aquatic environments [25]. We will also discuss the key factors for energy provided by nitrate conversion to remove Cd and Pi and in the responses of water temperature, EC, and pH to the switch of key factors in periphytic biofilm. Our study is a reference for contaminant removal when applying periphytic biofilm in water environments.

2. Materials and Methods

2.1. Preparation of Periphytic Biofilm

Periphytic biofilm was collected from the interface of water and soil in Nanjing, China, and cultured in a glass tank ($50 \text{ cm} \times 20 \text{ cm} \times 60 \text{ cm}$). An industrial soft carrier (Yixing Jineng Environmental Protection Co., Ltd., Yixing, China) was immersed in the water to

support the periphytic biofilm growth. The modified BG-11 medium (10 L, containing 0.2 g NaHCO_3 , 0.750 g $\text{MgSO}_4 \cdot 7\text{H}_2\text{O}$, 0.36 g $\text{CaCl}_2 \cdot 2\text{H}_2\text{O}$, 28.6 mg H_3BO_4 , 18.10 mg $\text{MnCl}_2 \cdot 4\text{H}_2\text{O}$, 2.2 mg ZnSO_4 , 3.90 mg Na_2MoO_4 , 0.790 mg $\text{CuSO}_4 \cdot 5\text{H}_2\text{O}$, 30 mg citric acid) was periodically added once every 2 weeks to provide the nutrient for the periphytic biofilm [26]. Three treatments were set up: NaNO_3 (10 mg L^{-1}) as excessive N treatment, KH_2PO_4 (5 mg L^{-1}) as excessive Pi treatment, and CdCl_2 (10 mg L^{-1}) as Cd pollution treatment. To reduce the influence of environmental conditions on the growth of the periphytic biofilm, the glass tank was kept in a greenhouse with a temperature maintained at 30/25 °C day/night, humidity being 65% [10]. After 60 days, periphytic biofilm grew on the carrier and formed a dense and stable biofilm (Figure S1). The periphytic biofilm was then ready for the subsequent experiments.

2.2. Experimental Treatments

Four experimental treatments were designed to examine the capacity of periphytic biofilms to reduce Cd concentrations under daily (Experiment I) and monthly (Experiment II) timescales. The treatments comprised four groups: (1) a control group containing only periphytic biofilm (PO); (2) a group with added electrons (10 V) based on the control (PE); (3) a group with supplementary photons based on the control (PL); and (4) a combination treatment with both electrons and photons added to the control (PEL) (Table 1). Each treatment was performed in triplicate. To initialize the periphytic biofilm treatments, an equal inoculum of 20 mL periphytic biofilm suspension was introduced into each experimental unit. To counteract evaporative water loss, tap water was replenished daily to maintain a consistent water level of 2–3 cm in all glass tanks.

Table 1. Experiment conditions and treatments.

Group	Treatment	Electricity (10 V) (Electrons)	Light (100 W) (Photons)
	PO	-	-
	PE	+	-
	PL	-	+
	PEL	+	+

Note: +, the selected treatment was added; and -, the selected treatment was not added.

2.3. Experimental Processes

Experiment I: Daily Process

Water samples were collected and water quality parameters such as TN, $\text{NO}_3\text{-N}$, T, and EC of the water samples in the apparatus were monitored for daily changes. The daily change experiment started on 20 September 2022, and water samples were collected every 6 h at 14:00, 20:00, 00:00, 06:00, and 14:00 on the next day (ND). All experiments were repeated three times.

Experiment II: Monthly Process

In this part, water quality-related parameters such as pH, TN, $\text{NO}_3\text{-N}$, temperature, and conductivity of the water samples in the equipment were monitored for monthly changes. The experiment started on 20 September 2022, and water samples were collected at 0d, 7d, 15d, and 30d. The experiment was repeated three times. The treatment device is shown in Figure S1.

2.4. Experimental Index

2.4.1. Measurement of pH, Temperature, and Electrical Conductivity (EC)

At each time point, 100 mL of water sample was taken from each glass slot using a syringe. After water sample collection, 100 mL of deionized water was added to each glass slot to maintain a constant volume [27]. The pH of the water sample was measured using a pH meter (PHSJ-3F, INESA Scientific Instrument Co., Ltd., Shanghai, China). The

temperature and EC were measured on-site using a YSI PRO 1020 water quality analyzer (YSI, Yellow Springs, OH, USA) [28].

2.4.2. Measurement of TN and NO_3^- -N

After water sample collection, 100 mL of deionized water was added to each glass slot to maintain a constant volume. TN and NO_3^- -N were determined using the potassium persulfate digestion-UV spectrophotometry method with a UV2355 UV spectrophotometer (Unico Co., Ltd., Shanghai, China) [29].

2.4.3. Cd and Pi Concentrations Determination

In the daily variation experiment, water samples were collected every 6 h at 14:00, 20:00, 00:00, 06:00, and 14:00 on the next day (ND). In the monthly variation experiment, water samples were collected at 0d, 7d, 15d, and 30d after the experiment initiation. Water samples were acidified with 3 mL of concentrated HCl and 1 mL of HNO_3 and heated in a water bath at 100 °C. Periphytic biofilms were sampled at the end of experiment, dried, and digested with a mixture of HCl, HNO_3 , and HClO_4 (4.50:1.50:5.00 mL) in glass tubes for 2.5 h at 220 °C. The Cd concentration in the digested solution was determined by ICP-MS (NEXION300XX, PerkinElmer, Inc., Waltham, MA, USA) [10].

2.5. Statistical Analysis

Data analysis was performed using Excel 2016 and SPSS 19.0 (IBM, USA). Student's *t*-tests were conducted to determine statistically significant differences between the control and treatment groups at a 0.05 significance level (Duncan's test). Each treatment constituted an independent experimental condition with three biological replicates. All chemical reagents utilized were of analytical grade and obtained from McLean Biochemical Technology Co., Ltd. (Shanghai, China).

3. Results

3.1. The Dynamics of Temperature, EC, and pH

In the daily experiment, distinct diurnal patterns of water temperature were observed across the various experimental treatments. Specifically, during the first 6 h from 14:00 to 20:00, temperature exhibited an increasing trend in the PO and PEL treatments, reaching a maximum of 21.0 °C under the PO condition. This was followed by a decline in temperature across all treatments (PO, PE, PL, and PEL) over the subsequent 10-h period from 20:00 to 8:00 the next day. The minimum temperature of 19.2 °C was recorded in the PEL treatment group during this phase. Subsequently, a rebound increase in temperature occurred in all treatments, with the PO treatment registering the highest temperature of 20.2 °C at the 24-h mark (Figure 1A).

In the monthly experiment, temperature fluctuations followed a more prolonged trajectory: an initial decline over the first 7 days was followed by a rise in the PL and PEL treatment groups peaking at 20.7 °C under PEL over days 8 to 15. Thereafter, a decreasing trend was observed across all treatment groups, with the maximum temperature attained in the PO treatment group by day 30 (Figure 1B).

Across both experimental timescales, the PEL treatment group consistently exhibited the lowest mean temperature of 19.3 °C (daily) and 18.5 °C (monthly). In contrast, the PO treatment group registered the highest temperatures at the conclusion of both experiments. These thermal dynamics constitute salient factors when evaluating experimental outcomes and treatment effects over time.

In the daily experiment, electrical conductivity (EC) exhibited complex dynamics across the different treatments over time. Initially, EC showed a smooth increasing trend over the first 18 h from 14:00 to 8:00 the next day (ND) in the P and PEL treatments, followed by a decline at 18 h specifically under the PEL condition. In contrast, the PE treatment group displayed a gradual EC increase, while EC was stable in the PL treatment group at 406.8 $\mu\text{S cm}^{-1}$ (Figure 1C).

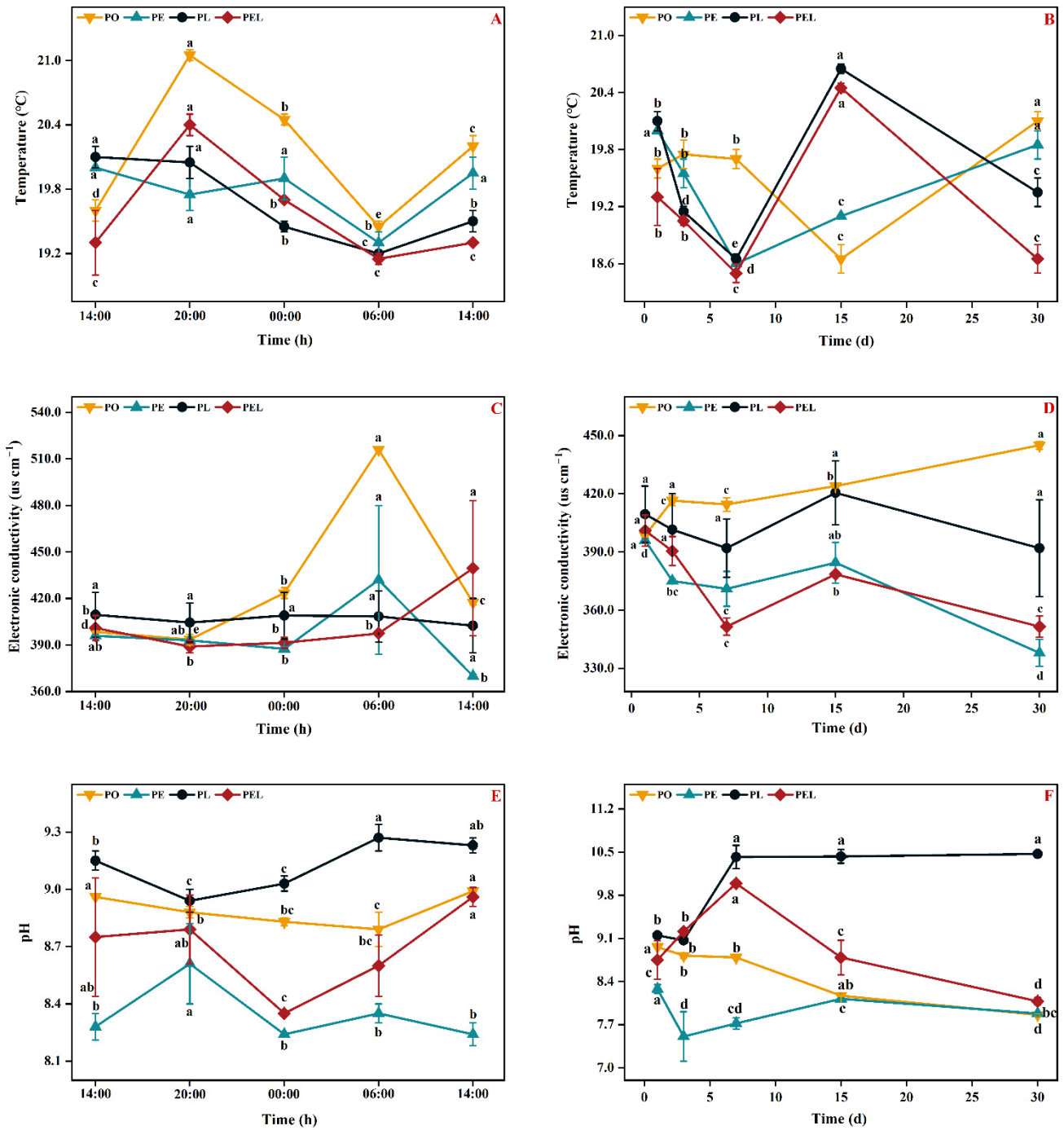


Figure 1. Temperature change over time under different treatments with (A) daily change and (B) monthly change; electrical conductivity changes over time under different treatments with (C) daily change and (D) monthly change; hydrogen ion concentration changes over time under different treatments with (E) daily change and (F) monthly change. (Note, PO, Periphyton only; PE, Periphyton treated with electricity; PL, Periphyton treated with light; and PEL, Periphyton treated with electricity and light. Different letters indicate significant differences between treatments ($p < 0.05$)).

In the monthly trial, EC rapidly rose within the first 3 days and continued increasing slowly thereafter in the P treatment. However, the other three treatments (PE, PL, and PEL) experienced a gradual EC reduction over 30 days, with PE registering the lowest EC by day 30 (Figure 1D). Within the daily timeframe, PEL yielded the maximum EC, while its EC significantly decreased ($p < 0.005$) over the monthly period. Ultimately, the PO treatment group exhibited the highest EC of $419 \mu\text{S cm}^{-1}$ after 30 days.

The pH exhibited significant differences across the PO, PE, PL, and PEL treatment groups over time. In the daily experiment, PL registered the highest pH of 10.4 at 24 h, while PO maintained a stable pH of 8.7. Under PEL, the pH trended upward in the first 6 h (14:00–20:00), decreased over the next 6 h, and rose again subsequently. In contrast, the pH declined in the PE treatment group (Figure 1E).

In the monthly trial, the PL condition sustained the highest pH of 10.4 from day 7 onwards. The P and PE treatments displayed opposite pH changes during the first 7 days but converged to the same value of 7.9 by day 30. Overall, the pH increased initially then decreased by day 30 in the P, PE, and PEL groups. The maximum pH values of 10.47 (daily) and 9.21 (monthly) were attained in the PL media, while PE registered the lowest pH across all treatments and time points (Figure 1F).

3.2. The Response of N Conversion

In the daily treatments, total nitrogen (TN) concentrations remained stable at 9.51 and 7.15 mg L^{-1} in the PO and PEL conditions over 24 h, respectively. Under PL, TN exhibited a declining trend, reaching 8.67 mg L^{-1} at 24 h. In the PE treatment group, TN first decreased then rebounded back to 8.67 mg L^{-1} at 24 h (Figure 2A).

In the monthly experiment, a significant decreasing TN trend was observed across all four treatment groups (Figure 2B). Specifically, TN declined gradually within the first 7 days in the PO and PEL groups, while steep drops occurred in the first 3 days under PE and PL. At 24 h, PL registered the lowest TN level of 8.67 mg L^{-1} . Over 30 days, the percent reductions in TN were 19.46%, 36.56%, 64.20%, and 27.30% for PO, PE, PL, and PEL, respectively. Overall, TN decreased significantly ($p < 0.05$) in the PE and PL treatment groups daily, reaching minimum concentrations of 3.70 and 3.26 mg L^{-1} after 30 days, respectively.

In the PL and PEL daily treatment groups, nitrate nitrogen (NO_3^- -N) concentrations remained stable at 5.60 and 5.24 mg L^{-1} , respectively, over 24 h. Under PE and PO conditions, NO_3^- -N increased within 24 h, reaching maximum values of 5.31 and 5.07 mg L^{-1} , respectively (Figure 2C).

In the first 7 days of the monthly treatments, NO_3^- -N was relatively constant around 4.93 , 4.93 , 5.54 , and 5.08 mg L^{-1} in the PO, PE, PL, and PEL groups, respectively. Thereafter, from day 15 onwards, a significant declining trend ($p < 0.05$) in NO_3^- -N was observed. By day 30, the percent reductions in NO_3^- -N were 27.50%, 57.23%, 77.64%, and 59.30% under PO, PE, PL, and PEL, respectively (Figure 2D). PE and PL exhibited similar NO_3^- -N trajectories over 30 days, ending with the lowest final NO_3^- -N concentrations. In contrast, NO_3^- -N remained stable in the PO treatment group.

3.3. The Pi and Cd Concentrations in the Water

In the daily experiment, phosphorus (Pi) concentration exhibited a stable increasing trend in the PO treatment group over 24 h, reaching 4.96 mg L^{-1} . In contrast, Pi declined in the other three treatments of PE, PL, and PEL, with final concentrations of 0.32 , 2.09 , and 0.16 mg L^{-1} , respectively, at 24 h (Figure 3A).

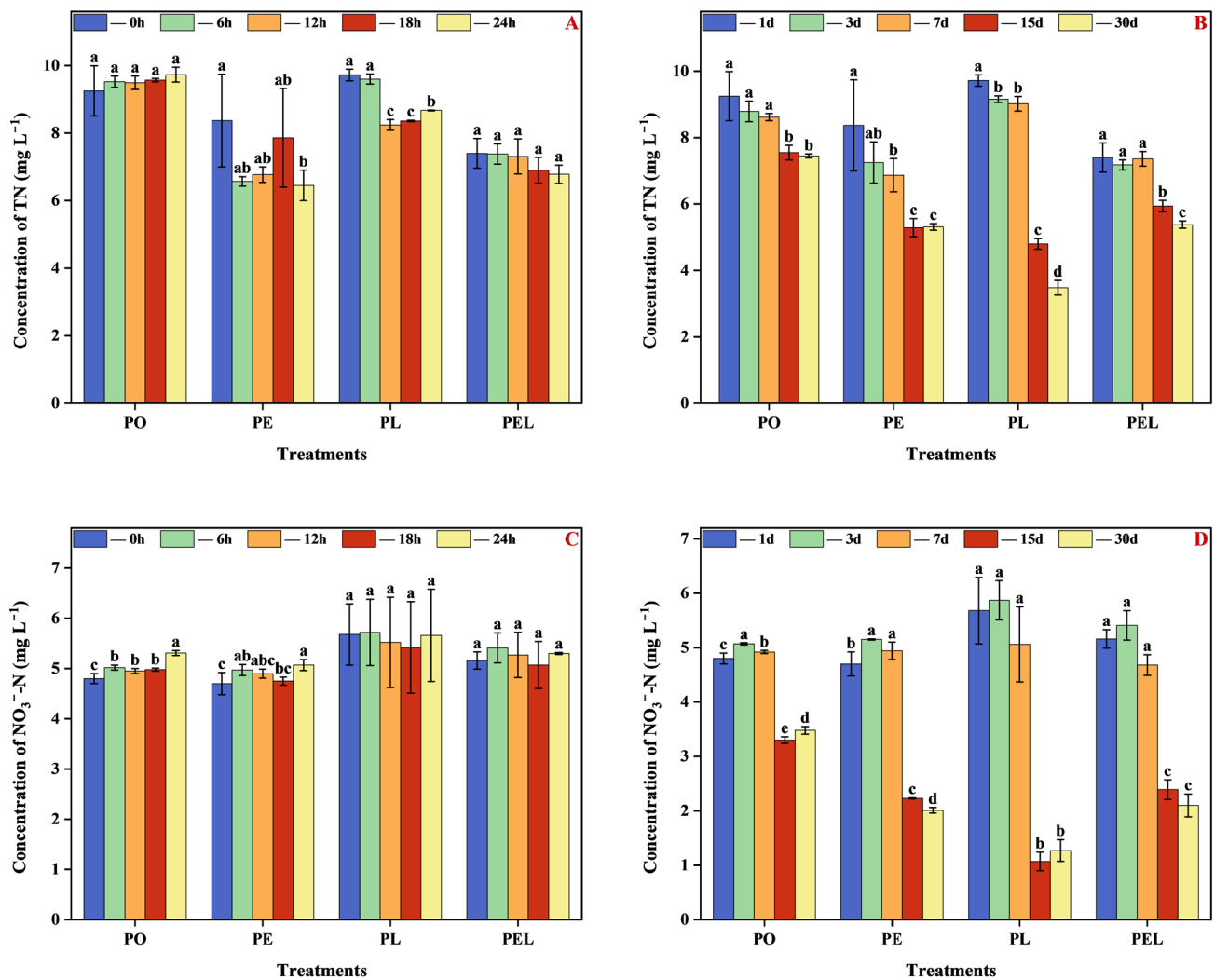


Figure 2. Concentration of TN in solution under different treatments with (A) daily change and (B) monthly change; concentration of NO₃⁻-N in solution under different treatments with (C) daily change and (D) monthly change. (Note, PO, Periphyton only; PE, Periphyton treated with electricity; PL, Periphyton treated with light; and PEL, Periphyton treated with electricity and light. Different letters indicate significant differences between treatments ($p < 0.05$)).

Meanwhile, the aqueous cadmium (Cd) level remained stable around 5.49 mg L⁻¹ under the PL condition. In the PE and PEL treatment groups, Cd was stable at 1.55 and 0.89 mg L⁻¹ over the first 18 h before declining thereafter. In the PO treatment group, Cd decreased continuously over 24 h, ending at 9.24 mg L⁻¹ (Figure 3C).

In the context of our monthly experimentation, it is noteworthy that there exists a statistically significant decline ($p < 0.05$) in the concentrations of both phosphorus (Pi) and cadmium (Cd) across all treatment regimens over a 30-day aqueous exposure period (depicted in Figure 3B,D). Specifically, the concentrations of Pi and Cd exhibit a stabilization phase commencing on the 3rd day of exposure within the PE, PL, and PEL treatment groups. Ultimately, after this stabilization phase, the final concentrations of phosphorus (Pi) and cadmium (Cd) were recorded as 0.13 and 0.15 mg L⁻¹, 0.14 mg L⁻¹, and 0.16 mg L⁻¹, and 0.01 and 0.21 mg L⁻¹, respectively, within these respective treatment categories. Importantly, after the culmination of the 30-day treatment period, phosphorus (Pi) and cadmium (Cd) levels exhibited a remarkable reduction of only 37.03% and 1.36%, respectively.

To evaluate periphytic biofilm accumulation under the different treatments, biomass was quantified on day 30 of the experiment. The recorded periphytic biofilm biomass values

were 0.62, 0.13, 1.63, and 0.44 g in the PO, PE, PL, and PEL treatment groups, respectively (Figure 4A). The final phosphorus (Pi) concentrations in the biofilm were 1.06, 0, 2.40, and 1.65 mg kg L⁻¹ under the PO, PE, PL, and PEL treatments. Meanwhile, the final cadmium (Cd) levels were 2.89, 0, 4.70, and 3.78 mg kg L⁻¹, respectively (Figure 4B,C).

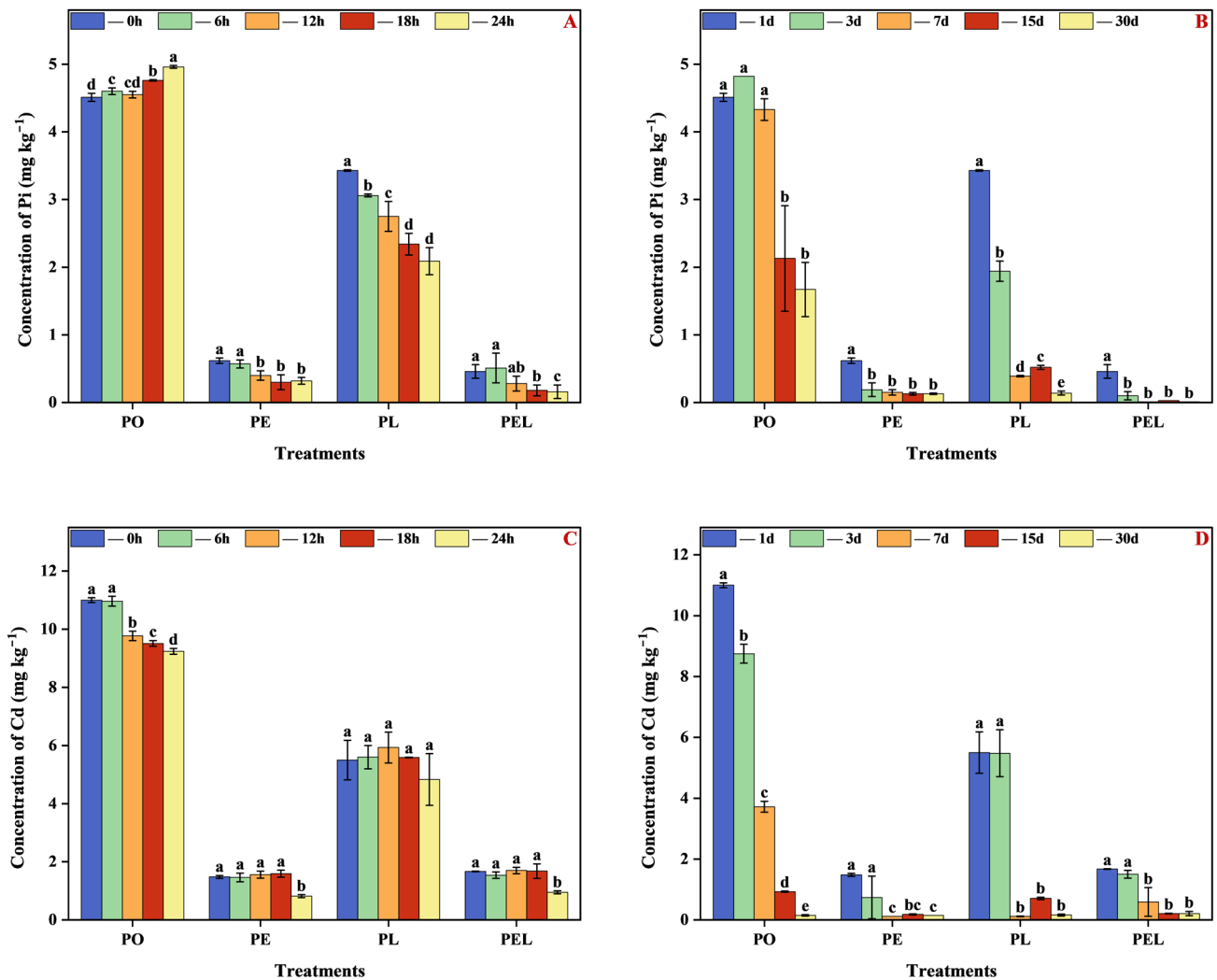


Figure 3. Concentration of Pi in solution under different treatments with (A) daily change and (B) monthly change; concentration of Cd in solution under different treatments with (C) daily change and (D) monthly change in media of different treatments. (Note, PO, Periphyton only; PE, Periphyton treated with electricity; PL, Periphyton treated with light; and PEL, Periphyton treated with electricity and light. Different letters indicate significant differences between treatments ($p < 0.05$)).

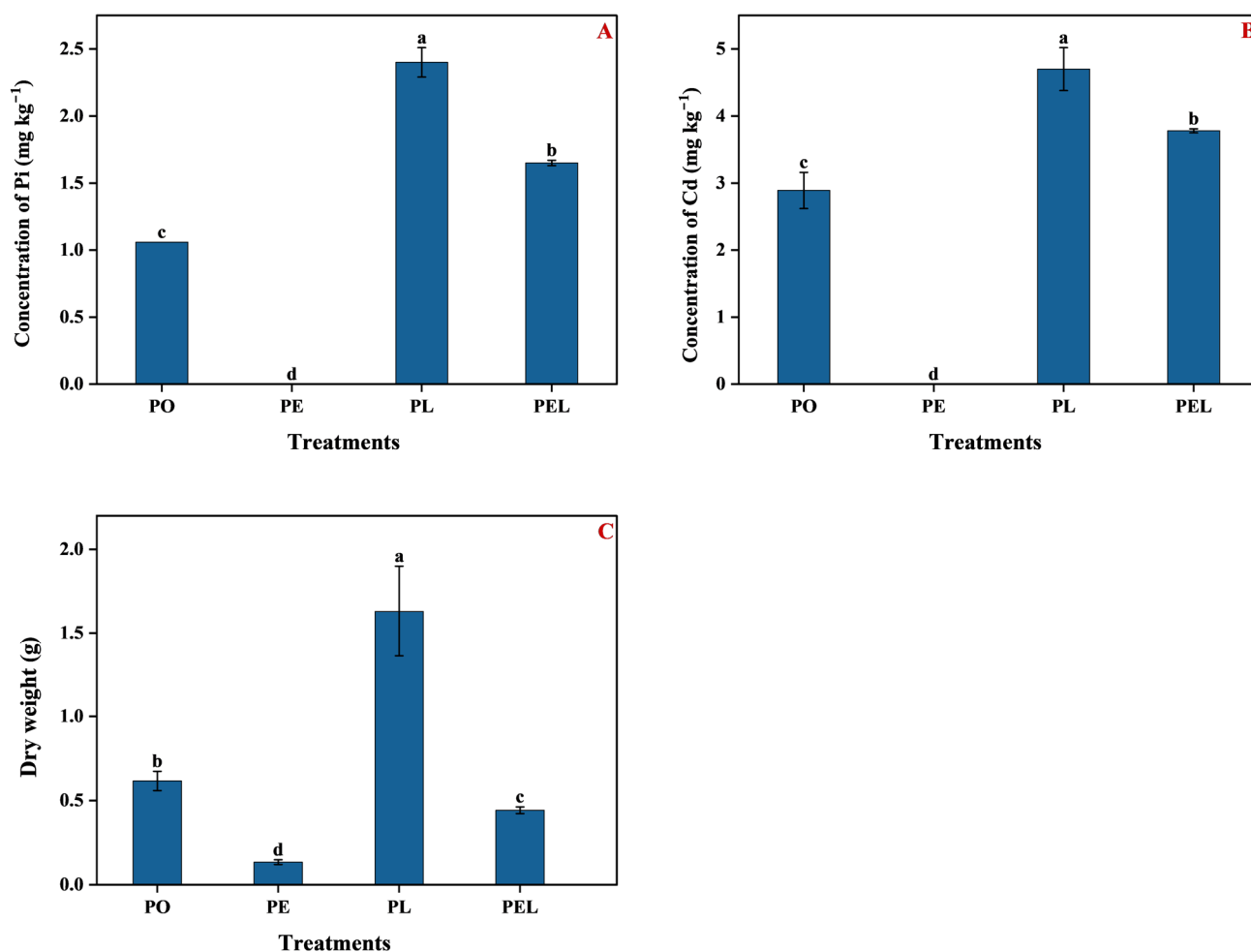


Figure 4. Contents of phosphorus (A) and cadmium (B) in the Periphyton after 4 weeks' treatment; and (C) the dry weight of periphyton under different treatments. (Note, PO, Periphyton only; PE, Periphyton treated with electricity; PL, Periphyton treated with light; and PEL, Periphyton treated with electricity and light. Different letters indicate significant differences between treatments ($p < 0.05$)).

4. Discussion

4.1. Performance of Photon and Electron in Contaminant Removal and Nitrate Conversion

Based on the monthly experiments, the PO treatment group exhibited the highest phosphorus (Pi) and cadmium (Cd) removal capacity per unit biomass, at $0.66 \mu\text{g Pi}$ and $1.78 \mu\text{g Cd}$. The addition of photons in the PL treatment group enhanced removal to $2.40 \mu\text{g Pi}$ and $4.70 \mu\text{g Cd}$ per unit, with total accumulations of $3.92 \mu\text{g Pi}$ and $7.66 \mu\text{g Cd}$. However, the incorporation of electrons in the PE treatment group significantly inhibited Pi and Cd uptake, resulting in no measurable accumulation. The combined electron and photon treatment PEL yielded the lowest uptake, at $0.73 \mu\text{g Pi}$ and $1.67 \mu\text{g Cd}$ per unit. These results indicate that individually elevating electron or photon levels does not augment Pi and Cd accumulation in periphytic biofilm. Moreover, the interactive effects of simultaneous electron and photon addition failed to improve contaminant removal. This implies that the combined electron and photon treatment may have disrupted pathways in the periphytic biofilm related to Pi and Cd uptake and sequestration.

Nitrate and ammonium conversion involve energy-dependent processes that are vital for biological transformations and nitrogen cycling [30,31]. In this study, the addition of electrons in the PE and PEL daily treatment groups significantly decreased total nitrogen (TN) concentrations, while photons did not impact TN. Over 30 days, electrons reduced

TN by 45.5%, but photons led to a greater 77.56% TN decrease in the monthly treatments, yielding the lowest final TN concentration of 1.27 mg L^{-1} across treatments. Nitrate nitrogen (NO_3^- -N) was initially stable in the first 24 h and 7 days, then declined markedly, with photons exerting a stronger effect than electrons in the PL and PE groups, respectively.

Regarding contaminant removal, these results imply that photons may stimulate nitrate and ammonium conversion, thereby enhancing periphytic biofilm accumulation of phosphorus (Pi) and cadmium (Cd). In contrast, electrons had a weaker influence on nitrate conversion based on the smaller TN and NO_3^- -N reductions observed monthly. Environmental factors like photons and electrons play critical roles in driving these energy-dependent conversions and nitrogen cycling, which consequently impact Pi and Cd removal by periphytic biofilms. Further discussion on how supplemental photons and electrons influence Pi and Cd uptake in contaminated systems by modulating periphytic biofilm processes is warranted.

4.2. The Environmental Factors Response after the Addition of Photon and Electron

The addition of electrons elevated the media temperature compared to photons in the PE treatment group; however, the temperature was highest with PO by the end (Figure 1A,B). Electrons did not impact electrical conductivity (EC) or pH, while supplemental photons significantly ($p < 0.05$) increased EC above $510 \mu\text{S cm}^{-1}$ and pH over 9.0 (Figure 1C–F). After 30 days, neither photons nor electrons further raised temperature or EC, although electrons increased temperature more than photons via periphytic biofilm growth (Figure 1B,D). Notably, added photons substantially elevated pH to 10.5 through periphytic biofilm by day 30 (Figure 1F).

In nitrate conversion, hydrogen protons are required, and photons may assist periphytic biofilms in absorbing more protons to accelerate nitrification, reflected in the $>15\%$ pH increase (Figure 1E,F) [32]. Previous studies report periphytic biofilms can reduce ammonia in May (longer daylight) via nitrification promotion [33], and increase pH and EC during stream revitalization in spring (longer days) in Krka National Park [34]. Our data align with these findings, demonstrating that supplemental photons elevated pH and EC through periphytic biofilms (Figure 1) and improved contaminant removal. Additionally, periphytic biofilms have reduced total nitrogen by 18% and ammonium by 72% alongside higher biological oxygen demand in wastewater treatment [35]. Enhanced light has also been shown to improve periphytic biofilm growth and subsequent nitrate and ammonium removal [22]. Our results agree that greater photon-stimulated periphytic growth significantly ($p < 0.05$) lowered total nitrogen by 64.20%, nitrate by 77.64%, and ammonium by 45.30% after 30 days (Figures 2 and S2). Collectively, these data indicate photons play a key role in improving physical conditions and contaminant removal through periphytic biofilms.

In this study, electrons exhibited no significant effects on electrical conductivity (EC) and pH increase. In contrast, photons significantly increased EC by 2.76% and pH by 2.12%, while maintaining lower temperatures relative to other treatments. After 30 days, neither photons nor electrons alone positively influenced temperature or EC rise. However, electrons showed a greater capacity to increase temperature versus photons through periphytic biofilm growth. Comparatively, photons led to higher EC levels than either electrons or the combination of electrons and photons. Moreover, supplemental photons markedly elevated pH through periphytic biofilm activity.

In nitrate conversion biochemical pathways, hydrogen protons are required, and photons may assist periphytic biofilms in absorbing more protons to accelerate nitrification, as evidenced by the $>14.43\%$ increase in media pH observed here. Aligning with previous findings, our data showed periphytic biofilm cultivated under longer daylight hours reduced ammonia and enhanced pH by 4.27% and EC by 2.76% during stream revitalization. Additionally, in wastewater treatment, periphytic biofilms have lowered total nitrogen and ammonium alongside higher biological oxygen demand. As an essential factor influencing periphytic biofilms, light promotes growth and subsequent nitrate and

ammonium removal. Corroborating these prior studies, our results confirm increased photon exposure improved periphytic biofilm growth, conferring significant reductions in total nitrogen, nitrate, and ammonium. Collectively, these data highlight photons as vital players in ameliorating physical conditions and contaminant levels in media via facilitation of periphytic biofilm activity.

4.3. Comparison of the Use of Photons and Electrons as a Biological Force

Light can be separated into photons and electrons, both critical particles in biological processes. It is reported that photoexcited electrons can induce electron-signal separation on periphytic biofilm surfaces, subsequently transmitted to cells [36]. Electron application in plant growth dates back to 1902 [37], although the mechanisms remain complex. Traditionally, electrons feature prominently in photosynthesis [38]. Studies show exogenous allelochemicals can boost leaf electron levels; however, excess electrons transfer as heat and damage cells [39]. Meanwhile, carbon dots added to leaves improve light-harvesting, conversion, and electron-donation in chloroplasts [40], enhancing light-electron transfer and photosynthesis when incorporated into leaf cells [41]. This suggests transferred electrons may be more beneficial than direct electrons. Unlike electrons, photons can directly stimulate chloroplasts, likely explaining the greater periphytic biofilm biomass increase with supplemental photons (Figure 4).

In contaminated conditions, the addition of electrons did not confer appreciably greater improvements in periphytic biofilm phosphorus (Pi) and cadmium (Cd) uptake (79.03% and 89.86% removal, respectively) compared to the control (Figure 3). In Pi removal by periphytic biofilms, adsorption is the major mechanism [42], and excess electrons may impede this physical process. For Cd, adsorption and immobilization by organic matter on periphytic biofilm surfaces and in the media are key [10], which electron addition could hinder by reducing positive adsorption sites. This explains the limited contribution of supplemented electrons to Pi and Cd removal. In contrast, added photons enhanced uptake by increasing periphytic biofilm growth, enabling photons to improve Pi and Cd removal.

Given the capabilities of periphytic biofilms in regulating pollutant removal, photon-based technologies warrant further research across various aspects. Key areas needing exploration include elucidating mechanisms like interactions between photon addition and periphytic biofilms, examining effects on constituent organisms (e.g., bacteria, algae, fungi), and deciphering underlying processes. Another critical facet is investigating alterations in surrounding biological community characteristics, including impacts on periphytic biofilm biodiversity, population density, and community structure. Moreover, changes in extracellular polymers that mediate microbial aggregation and substrate adhesion necessitate study, specifically regarding how photonic technology parameters like light intensity, wavelength, and interactions with environmental factors (temperature, oxygen) affect polymers. Ultimately, comprehensive understanding of photonic-periphytic biofilm interactions involving characterization of community-level changes, decrypting mechanisms, and defining optimal photon delivery conditions is required to engineer and implement this technology for enhanced pollutant removal in aquatic systems.

Finally, applied studies are imperative to evaluate the potential of photon addition technology across diverse environments, including different water types (freshwater, seawater, wastewater) and its effectiveness in removing various pollutants such as organic contaminants and heavy metals. Advancing research across these key dimensions will augment our fundamental comprehension of photon-periphytic biofilm interactions and underpin the translation of photon-based technologies to engineer periphytic biofilms for enhanced removal of aquatic pollutants. Ultimately, a synergistic approach combining mechanistic studies to elucidate interactions, community-level characterizations, and applied assessments across water environments and contaminant types will unlock the immense possibilities of periphytic biofilm-photon technology pairings for next-generation water treatment systems.

5. Conclusions

This study provides important insights into the performance of photons and electrons in contaminant removal and their influences on environmental factors. We found that while 10 V electron addition had minimal impacts on contaminant accumulation, 4000 lux photons significantly promoted nitrate and ammonium conversion and enhanced cadmium and phosphorus uptake to 4.70 and 2.40 mg kg⁻¹ in periphytic biofilm, respectively. Additionally, temperature, electrical conductivity, and pH were differentially affected by electrons versus photons. These findings advance fundamental understanding of harnessing electrons and photons as biological drivers to boost contaminant removal efficiency by periphytic biofilms. Our results deliver valuable knowledge and strategies for applying these stimuli in water treatment and ecosystem management applications. Overall, elucidating the capabilities and mechanisms of periphytic biofilm manipulation using photon versus electron supplementation constitutes a vital step toward engineering next-generation aquatic remediation systems.

Supplementary Materials: The following supporting information can be downloaded at: <https://www.mdpi.com/article/10.3390/w15183314/s1>, Figure S1. Experimental device in progress; Figure S2. Concentration of NH₄⁺-N in solution under different treatments with (A) daily change and (B) monthly change in periphytic biofilm.

Author Contributions: Formal analysis, Y.S.; Funding acquisition, H.L.; Investigation, J.Z. and J.H.; Methodology, J.Z., Y.L. and H.H.; Resources, Y.Z.; Software, Y.S.; Supervision, Y.Z., J.H. and H.L.; Writing—original draft, J.Z., Y.L., Y.S. and H.H.; Writing—review and editing, J.L., Y.Z., J.H. and H.L. All authors will be informed about each step of manuscript processing including submission, revision, revision reminder, etc., via emails from our system or assigned Assistant Editor. All authors have read and agreed to the published version of the manuscript.

Funding: This research was funded by the National Natural Science Foundation of China (42277408), the Nature Science Foundation for Excellent Young Scholars of Jiangsu Province (BK20200057), Jiangsu Provincial Science and Technology Innovation Special Fund Project of Carbon Emission Peak and Carbon Neutralization (frontier and basis: BK20220016), the Basic Science (Natural Science) Project of Higher Education Institutions of Jiangsu Province (21KJB610012), the Talent Introduction Program of Nanjing Polytechnic Institute (NJPI-2021-03), and the Entrepreneurship and Innovation Program of Yunlong District in Xuzhou.

Data Availability Statement: The authors confirm that the data supporting the findings of this study are available within the article [and/or its supplementary materials].

Conflicts of Interest: The authors declare that they have no known competing financial interest or personal relationships that could have appeared to influence the work reported in this paper.

References

1. Huang, H.; Zhao, D.; Wang, P. Biogeochemical Control on the Mobilization of Cd in Soil. *Curr. Pollut. Rep.* **2021**, *7*, 194–200. [[CrossRef](#)]
2. Chen, L.; Zhou, M.; Wang, J.; Zhang, Z.; Duan, C.; Wang, X.; Zhao, S.; Bai, X.; Li, Z.; Li, Z.; et al. A global meta-analysis of heavy metal(loid)s pollution in soils near copper mines: Evaluation of pollution level and probabilistic health risks. *Sci. Total Environ.* **2022**, *835*, 155441. [[CrossRef](#)] [[PubMed](#)]
3. Li, C.; Wang, H.; Liao, X.; Xiao, R.; Liu, K.; Bai, J.; Li, B.; He, Q. Heavy metal pollution in coastal wetlands: A systematic review of studies globally over the past three decades. *J. Hazard. Mater.* **2022**, *424 Pt A*, 127312. [[CrossRef](#)]
4. Huang, B.-Y.; Lü, Q.-X.; Tang, Z.-X.; Tang, Z.; Chen, H.-P.; Yang, X.-P.; Zhao, F.-J.; Wang, P. Machine learning methods to predict cadmium (Cd) concentration in rice grain and support soil management at a regional scale. *Fundam. Res.* **2023**, *in press*. [[CrossRef](#)]
5. Yang, J.; Li, G.; Xia, M.; Chen, Y.; Chen, Y.; Kumar, S.; Sun, Z.; Li, X.; Zhao, X.; Hou, H. Combined effects of temperature and nutrients on the toxicity of cadmium in duckweed (*Lemna aequinoctialis*). *J. Hazard. Mater.* **2022**, *432*, 128646. [[CrossRef](#)] [[PubMed](#)]
6. Carpenter, S.R. Eutrophication of aquatic ecosystems: Bistability and soil phosphorus. *Proc. Natl. Acad. Sci. USA* **2005**, *102*, 10002–10005. [[CrossRef](#)]
7. Lu, H.; Qi, W.; Liu, J.; Bai, Y.; Tang, B.; Shao, H. Paddy periphytic biofilm: Potential roles for salt and nutrient management in degraded mudflats from coastal reclamation. *Land Degrad. Dev.* **2018**, *29*, 2932–2941. [[CrossRef](#)]
8. Balle, M.G.; Ferragut, C.; Coelho, L.H.G.; Jesus, T.A.d. Phosphorus and metals immobilization by periphytic biofilm in a shallow eutrophic reservoir. *Acta Limnol. Bras.* **2021**, *33*, e11. [[CrossRef](#)]

9. Marella, T.K.; Saxena, A.; Tiwari, A.; Datta, A.; Dixit, S. Treating agricultural non-point source pollutants using periphytic biofilm biofilms and biomass volarization. *J. Environ. Manag.* **2022**, *301*, 113869. [[CrossRef](#)] [[PubMed](#)]
10. Lu, H.; Dong, Y.; Feng, Y.; Bai, Y.; Tang, X.; Li, Y.; Yang, L.; Liu, J. Paddy periphytic biofilm reduced cadmium accumulation in rice (*Oryza sativa*) by removing and immobilizing cadmium from the water-soil interface. *Environ. Pollut.* **2020**, *261*, 114103. [[CrossRef](#)] [[PubMed](#)]
11. Zhong, W.; Zhao, W.; Song, J. Responses of Periphytic biofilm Microbial Growth, Activity, and Pollutant Removal Efficiency to Cu Exposure. *Int. J. Environ. Res. Public Health* **2020**, *17*, 941. [[CrossRef](#)] [[PubMed](#)]
12. Yang, J.; Tang, C.; Wang, F.; Wu, Y. Co-contamination of Cu and Cd in paddy fields: Using periphytic biofilm to entrap heavy metals. *J. Hazard. Mater.* **2016**, *304*, 150–158. [[CrossRef](#)]
13. Kilroy, C.; Brown, L.; Carlin, L.; Lambert, P.; Sinton, A.; Wech, J.A.; Howard-Williams, C. Nitrogen stimulation of periphytic biofilm biomass in rivers: Differential effects of ammonium-N and nitrate-N. *Freshw. Sci.* **2020**, *39*, 485–496. [[CrossRef](#)]
14. Xiong, Q.; Hu, J.; Wei, H.; Zhang, H.; Zhu, J. Relationship between Plant Roots, Rhizosphere Microorganisms, and Nitrogen and Its Special Focus on Rice. *Agriculture* **2021**, *11*, 234. [[CrossRef](#)]
15. Lee, K.H.; Jeong, H.J.; Kang, H.C.; Ok, J.H.; You, J.H.; Park, S.A. Growth rates and nitrate uptake of co-occurring red-tide dinoflagellates *Alexandrium affine* and *A. fraterculus* as a function of nitrate concentration under light-dark and continuous light conditions. *Algae* **2019**, *34*, 237–251. [[CrossRef](#)]
16. Virsile, A.; Brazaityte, A.; Vastakaite-Kairiene, V.; Miliauskiene, J.; Jankauskiene, J.; Novickovas, A.; Lauzike, K.; Samuoliene, G. The distinct impact of multi-color LED light on nitrate, amino acid, soluble sugar and organic acid contents in red and green leaf lettuce cultivated in controlled environment. *Food Chem.* **2020**, *310*, 125799. [[CrossRef](#)]
17. Miyake, C.; Horiguchi, S.; Makino, A.; Shinzaki, Y.; Yamamoto, H.; Tomizawa, K. Effects of light intensity on cyclic electron flow around PSI and its relationship to non-photochemical quenching of Chl fluorescence in tobacco leaves. *Plant Cell Physiol.* **2005**, *46*, 1819–1830. [[CrossRef](#)]
18. Theerthagiri, J.; Park, J.; Das, H.T.; Rahamathulla, N.; Cardoso, E.S.; Murthy, A.P.; Choi, M.Y. Electrocatalytic conversion of nitrate waste into ammonia: A review. *Environ. Chem. Lett.* **2022**, *20*, 2929–2949. [[CrossRef](#)]
19. Huang, W.; Hu, H.; Zhang, S.B. Photorespiration plays an important role in the regulation of photosynthetic electron flow under fluctuating light in tobacco plants grown under full sunlight. *Front. Plant Sci.* **2015**, *6*, 621. [[CrossRef](#)]
20. Wu, Y.; Yang, J.; Tang, J.; Kerr, P.; Wong, P.K. The remediation of extremely acidic and moderate pH soil leachates containing Cu (II) and Cd (II) by native periphytic biofilm. *J. Clean. Prod.* **2017**, *162*, 846–855. [[CrossRef](#)]
21. Gao, X.; Wang, Y.; Sun, B.; Li, N. Nitrogen and phosphorus removal comparison between periphytic biofilm on artificial substrates and plant-periphytic biofilm complex in floating treatment wetlands. *Environ. Sci. Pollut. Res. Int.* **2019**, *26*, 21161–21171. [[CrossRef](#)] [[PubMed](#)]
22. Bécares, E.; Gomá, J.; Fernández-Aláez, M.; Fernández-Aláez, C.; Romo, S.; Miracle, M.R.; Ståhl-Delbanco, A.; Hansson, L.-A.; Gyllström, M.; Van de Bund, W.J.; et al. Effects of nutrients and fish on periphytic biofilm and plant biomass across a European latitudinal gradient. *Aquat. Ecol.* **2007**, *42*, 561–574. [[CrossRef](#)]
23. Pacheco, J.P.; Aznarez, C.; Levi, E.E.; Baattrup-Pedersen, A.; Jeppesen, E. Periphytic biofilm responses to nitrogen decline and warming in eutrophic shallow lake mesocosms. *Hydrobiologia* **2021**, *849*, 3889–3904. [[CrossRef](#)]
24. Stevenson, R.J.; Bennett, B.J.; Jordan, D.N.; French, R.D. Phosphorus regulates stream injury by filamentous green algae, DO, and pH with thresholds in responses. *Hydrobiologia* **2012**, *695*, 25–42. [[CrossRef](#)]
25. Schiller, D.V.; Martí, E.; Riera, J.L.; Sabater, F. Effects of nutrients and light on periphytic biofilm biomass and nitrogen uptake in Mediterranean streams with contrasting land uses. *Freshw. Biol.* **2007**, *52*, 891–906. [[CrossRef](#)]
26. Lu, H.; Feng, Y.; Wang, J.; Wu, Y.; Shao, H.; Yang, L. Responses of periphytic biofilm morphology, structure, and function to extreme nutrient loading. *Environ. Pollut.* **2016**, *214*, 878–884. [[CrossRef](#)]
27. Hua, C.; Li, C.; Jiang, Y.; Huang, M.; Williamson, V.M.; Wang, C. Response of soybean cyst nematode (*Heterodera glycines*) and root-knot nematodes (*Meloidogyne* spp.) to gradients of pH and inorganic salts. *Plant Soil* **2020**, *455*, 305–318. [[CrossRef](#)]
28. Liu, W.; Tan, Q.; Chu, Y.; Chen, J.; Yang, L.; Ma, L.; Zhang, Y.; Wu, Z.; He, F. An integrated analysis of pond ecosystem around Poyang Lake: Assessment of water quality, sediment geochemistry, phytoplankton and benthic macroinvertebrates diversity and habitat condition. *Aquat. Ecol.* **2022**, *56*, 775–791. [[CrossRef](#)]
29. Peng, X.; Yi, K.; Lin, Q.; Zhang, L.; Zhang, Y.; Liu, B.; Wu, Z. Annual changes in periphytic biofilm communities and their diatom indicator species, in the littoral zone of a subtropical urban lake restored by submerged plants. *Ecol. Eng.* **2020**, *155*, 105958. [[CrossRef](#)]
30. Burgin, A.J.; Hamilton, S.K. Have we overemphasized the role of denitrification in aquatic ecosystems? A review of nitrate removal pathways. *Front. Ecol. Environ.* **2007**, *5*, 89–96. [[CrossRef](#)]
31. Galloway, J.N.; Townsend, A.R.; Erisman, J.W.; Bekunda, M.; Cai, Z.; Freney, J.R.; Martinelli, L.A.; Seitzinger, S.P.; Sutton, M.A. Transformation of the nitrogen cycle: Recent trends, questions, and potential solutions. *Science* **2008**, *320*, 889–892. [[CrossRef](#)] [[PubMed](#)]
32. DeMartino, A.W.; Kim-Shapiro, D.B.; Patel, R.P.; Gladwin, M.T. Nitrite and nitrate chemical biology and signalling. *Br. J. Pharmacol.* **2019**, *176*, 228–245. [[CrossRef](#)]

33. Azim, M.E.; Verdegem, M.C.J.; Khatoon, H.; Wahab, M.A.; van Dam, A.A.; Beveridge, M.C.M. A comparison of fertilization, feeding and three periphytic biofilm substrates for increasing fish production in freshwater pond aquaculture in Bangladesh. *Aquaculture* **2002**, *212*, 227–243. [[CrossRef](#)]
34. Gulin, V.; Matoničkin Kepčija, R.; Sertić Perić, M.; Felja, I.; Fajković, H.; Križnjak, K. Environmental and periphytic biofilm response to stream revitalization—A Pilot study from a tufa barrier. *Ecol. Indic.* **2021**, *126*, 107629. [[CrossRef](#)]
35. Ogura, A.; Takeda, K.; Nakatsubo, T. Periphytic biofilm contribution to nitrogen dynamics in the discharge from a wastewater treatment plant. *River Res. Appl.* **2009**, *25*, 229–235. [[CrossRef](#)]
36. Zhu, N.; Tang, J.; Tang, C.; Duan, P.; Yao, L.; Wu, Y.; Dionysiou, D.D. Combined CdS nanoparticles-assisted photocatalysis and periphytic biological processes for nitrate removal. *Chem. Eng. J.* **2018**, *353*, 237–245. [[CrossRef](#)]
37. Luvisi, A. Electronic identification technology for agriculture, plant, and food. A review. *Agron. Sustain. Dev.* **2016**, *36*, 13. [[CrossRef](#)]
38. Yamori, W.; Shikanai, T. Physiological Functions of Cyclic Electron Transport Around Photosystem I in Sustaining Photosynthesis and Plant Growth. *Annu. Rev. Plant Biol.* **2016**, *67*, 81–106. [[CrossRef](#)]
39. Zhang, K.M.; Shen, Y.; Zhou, X.Q.; Fang, Y.M.; Liu, Y.; Ma, L.Q. Photosynthetic electron-transfer reactions in the gametophyte of *Pteris multifida* reveal the presence of allelopathic interference from the invasive plant species *Bidens pilosa*. *J. Photochem. Photobiol. B* **2016**, *158*, 81–88. [[CrossRef](#)]
40. Hallaji, Z.; Bagheri, Z.; Tavassoli, Z.; Ranjbar, B. Fluorescent carbon dot as an optical amplifier in modern agriculture. *Sustain. Mater. Technol.* **2022**, *34*, e00493. [[CrossRef](#)]
41. Wang, C.; Yang, H.; Chen, F.; Yue, L.; Wang, Z.; Xing, B. Nitrogen-Doped Carbon Dots Increased Light Conversion and Electron Supply to Improve the Corn Photosystem and Yield. *Environ. Sci. Technol.* **2021**, *55*, 12317–12325. [[CrossRef](#)] [[PubMed](#)]
42. Lu, H.; Yang, L.; Shabbir, S.; Wu, Y. The adsorption process during inorganic phosphorus removal by cultured periphytic biofilm. *Environ. Sci. Pollut. Res. Int.* **2014**, *21*, 8782–8791. [[CrossRef](#)] [[PubMed](#)]

Disclaimer/Publisher's Note: The statements, opinions and data contained in all publications are solely those of the individual author(s) and contributor(s) and not of MDPI and/or the editor(s). MDPI and/or the editor(s) disclaim responsibility for any injury to people or property resulting from any ideas, methods, instructions or products referred to in the content.